JOURNAL OF AIRCRAFT
Vol. 43, No. 2, March–April 2006

Engineering Notes

ENGINEERING NOTES are short manuscripts describing new developments or important results of a preliminary nature. These Notes should not exceed 2500 words (where a figure or table counts as 200 words). Following informal review by the Editors, they may be published within a few months of the date of receipt. Style requirements are the same as for regular contributions (see inside back cover).

Design, Fabrication, and Performance Test of a Rotary-Wing Micro Aerial Vehicle

Gyou Beom Kim,* Nam Seo Goo,† Kwang Joon Yoon,‡
Hoon Cheol Park,‡ and Yung H. Yu‡
Konkuk University, Seoul 143-701, Republic of Korea

I. Introduction

SINCE the early 1990s, research has been conducted on micro aerial vehicles (MAVs), which have dimensions of 15 cm or less, to assess potential commercial and military applications.[1] It has been shown that fixed-wing MAVs with wingspans as small as 13 cm can fly very well with cameras, which was thought to be impossible only 7 years earlier. Along with other developers, we also developed a 13-cm-wide, fixed-wing MAV Batwing in 2003.

Because fixed-wing MAVs are generally difficult to control, it is very difficult to reconnoiter a specific area precisely, and so only well-trained people can operate them. For surveillance uses, rotary-wing MAVs have demonstrated better performance in such operations as vertical takeoff, hovering capability, and low-speed flight.

There have been several studies on rotary-wing MAVs. The Micro Flying Robot, made by Seiko Epson, used one electric motor in a coaxial rotor system to eliminate an antitorque device.[2] A rotary-wing MAV, made by the University of Maryland, also uses a coaxial system and an electric motor.[3] Though coaxial rotor systems with counter-rotating blades cancel out torques, heavy and complicated gear systems are required to operate them.[4] Another concept, I-STAR, made by the Allied Aerospace Company, used a ducted fan.[5]

The authors have been developing a rotary-wing MAV with a single-rotor system since 2001. The 2002 model used one rotor blade, an electric motor, and fixed-angle antitorque vanes to eliminate torque caused by rotor rotation. Unfortunately, this MAV was so unstable that it could not fly for more than 5 s. It was found that the fixed-angle antitorque vanes did not perform properly.[6] To solve this problem, the 2003 model adopted a rotor blade and two control surfaces linked to a servomotor. The concept of an elevon was used to cancel out torque and to provide directional control. Although this MAV model was able to fly for approximately 1 min and was more stable than the 2002 model, the antitorque control device required further improvement.[6]

Presented as Paper 2004-6333 at the AIAA Unmanned Unlimited Technical Conference, Chicago, IL, 20–23 September 2004; received 17 March 2005; revision received 23 August 2005; accepted for publication 10 November 2005.

*Graduate Student, Department of Aerospace Engineering.
†Assistant Professor, Department of Aerospace Engineering; nsgoo@konkuk.ac.kr. Member AIAA.
‡Professor, Department of Aerospace Engineering.

Our goal was to develop an antitorque control system with a gyroscope, which is necessary for a single-rotor MAV. The MAV utilizes an electronic motor, a rotor with two blades, two passive and two active antitorque vanes, a directional control surface, an rf receiver, an electronic speed controller (ESC), a gyroscope, a lithium polymer battery, and carbon/epoxy rod struts. Performance tests showed that the antitorque control system produced sufficient torque for stable flight. Even though the weight of the MAV was below 120 g, the MAV could fly for approximately 5 min. The main advantage of this MAV is easy maneuvers due to enhanced stability with the antitorque control system. This Note describes the design, fabrication, and performance tests of the rotary-wing MAV powered by an electric motor.

II. Basic Concepts and Experiments

The governing equation of the body rotation caused by the rotation of a rotor blade can be written as:

$$I\ddot{\theta}_B = Q_{\text{anti}}(\Omega) - Q_{\text{vane}}(\Omega, \delta_c) \tag{1}$$

where I, θ_B, Q_{anti}, Q_{vane}, Ω, and δ_c refer to the second moment of inertia of a body, a body rotation angle, torque by the rotation of a rotor, torque by the lift of antitorque vanes, angular velocity, and a control angle of active vanes, respectively. A body rotation can be eliminated when a body can produce enough torque to negate the antitorque due to body rotation. In the passive control method, we used antitorque control vanes with a fixed-angle control surface, as in our 2002 model. Because rotational speeds of a rotor were different for various flight conditions, the passive control method did not work well. In the active control method, which is more promising, the torque was produced from the lift of the antitorque vanes, as in 2003 model.

We made three measurements: 1) thrust produced by rotor blades 2) torque due to blade rotation Q_{anti} and 3) induced velocity distribution under the rotor blade. The first measurement aimed to estimate the weight of the rotary-wing MAV. The second and third measurements were done to determine the optimal size and position for the antitorque vanes.

For comparison with the experimental results, the thrust of rotor can be calculated using the blade element theory[7,8] as follows:

$$T = \int_{r=0}^{r=R} b\frac{1}{2}\rho(\Omega r)^2 a(\theta - \varphi)c\,\mathrm{d}r \tag{2}$$

where b, ρ, a, θ, φ, c, and R refer to the number of blades, air density, lift coefficient, pitch angle, inflow angle, chord of the blade, and radius of the blade, respectively. For simplicity, we assumed that the inflow distribution was uniform along the blade span and that the blade had an ideal twist. Then, for a constant chord blade, the thrust of the rotor is

$$T = C_T \pi R^2 \rho(\Omega R)^2 \tag{3}$$

where

$$C_T = (\sigma/4)a(\theta_t - \varphi_t) \tag{4}$$

$$\sigma = bc/\pi R \tag{5}$$

where C_T, σ, and subscript t refer to the rotor thrust coefficient, solidity ratio, and value at the blade tip, respectively.

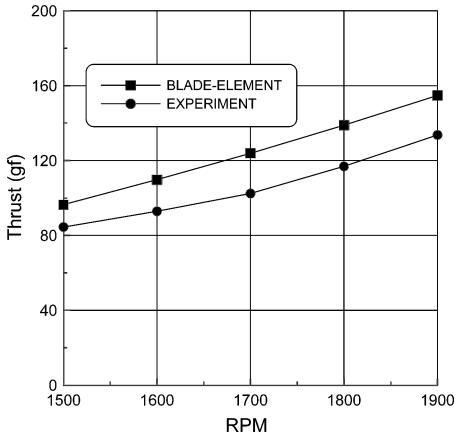

Fig. 1 Thrust vs RPM produced by rotor blade.

In a similar manner, the torque of the rotor can be written as

$$Q = C_Q \pi R^2 \rho (\Omega R)^2 R \tag{6}$$

where

$$C_Q = C_T^{\frac{3}{2}} / \sqrt{2} + \sigma\delta/8 \tag{7}$$

where δ refers to the average blade profile-drag coefficient. We used a commercial rotor blade with a tip pitch angle of about 14 deg. The equivalent chords for thrust and torque estimations were calculated based on the planform of the blade.

Thrust vs revolutions per minute (RPM) was measured with a test device consisting of a balance and a propulsion fixture jig. The height of the thrust test device was about 70 cm (twice the rotor diameter) to avoid the ground effect. Figure 1 shows the measured thrusts vs RPM graph, which was used for the weight estimation. At 1900 rpm, about 130 gf of thrust was measured, which is about 20% lower than the value calculated using the blade element theory. This result might be because the blade element theory results in higher values because it does not include losses.

Torque produced by the rotor was measured to design the shape of the antitorque vanes. Figure 2a shows the torque measurement device. When the rotor blade was rotated in the counterclockwise direction, the body of the motor tended to rotate clockwise. A wire attached to the motor pulled down a spring balance. The produced torque was calculated by multiplying the moment arm and the measured force. As shown in Fig. 2b, about 270 gf · cm of torque was measured at 1900 rpm, and this value is 16% larger than the value calculated using the blade element theory. The measured torque data were used to determine the area of antitorque vanes in Sec. III.B.

We measured the induced velocity to determine both the optimal position of antitorque vane attachment and the torque caused by the lift of the antitorque vanes. With an anemometer, we measured the profiles of the induced velocity at different positions under the rotor blade. The experiment was performed at a fixed rotational speed of 1900 rpm. The measured data, as shown in Fig. 3, show that the induced velocities had similar profiles for different positions under the rotor blade. With these data, we determined the optimal position of antitorque vanes.

III. Design, Fabrication, and Flight Test

A. Conceptual Design

Figure 4a shows the conceptual design shape of the Konkuk University 2004 MAV model. The system is composed of an electronic motor, a rotor with two blades, two passive antitorque vanes, two active antitorque vanes, a directional control surface, an rf receiver, an ESC, a gyroscope, a lithium polymer battery, and carbon/epoxy rod struts.

At 1900 rpm, which was the optimal RPM of the present electric motor, the measured thrust was 130 gf. This value of thrust limited our design to a total weight of less than 130 gf. The second column of Table 1 shows the weight of each component.

Table 1 Weight and current consumption estimates

Sub-system	Weight, gf	Current consumption
Power source	64	1.5 A
Control part	20	20 mA
Video part	5.5	150 mA
Structure	20.5	N.A.
Total	110	1.67 A

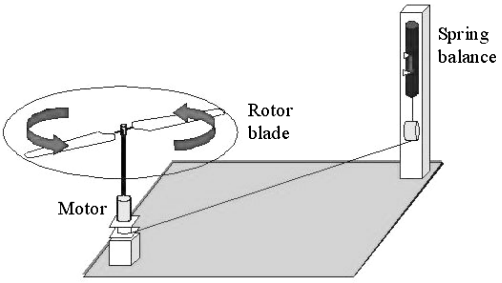

a) Schematic of test equipment

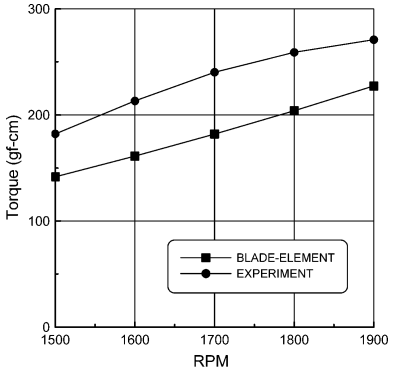

b) Measured torque vs RPM

Fig. 2 Measurement of torque due to blade rotation.

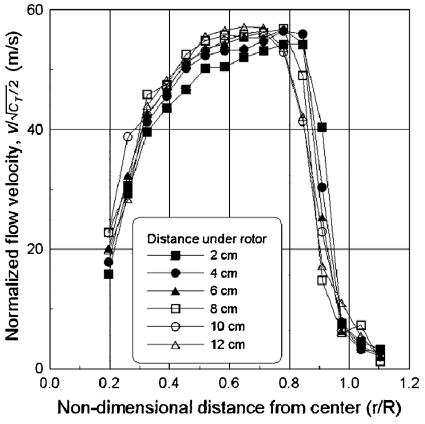

Fig. 3 Induced velocity profile at 1900 rpm.

The last column of Table 1 lists the estimated current consumption. The total necessary current was 1.67 A. In terms of current, the flight time could be estimated as follows:

$$340\ \text{mA} \cdot \text{h}/1.67\ \text{A} \times 0.7 = 0.14\ \text{h} = 8.4\ \text{min} \tag{8}$$

In this calculation, the power of the present battery was 340 mA · h, and the system efficiency was assumed to be 70%.

B. Antitorque Control System

The developed rotary-wing MAV had four antitorque vanes: two passive and two active, with antitorque control surfaces. At

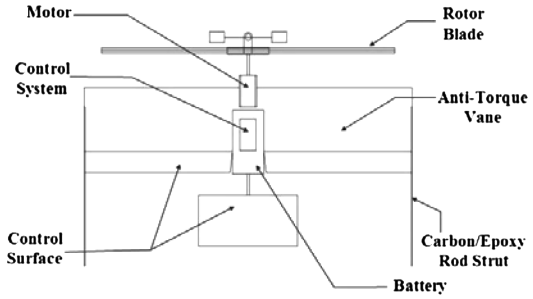

a) Conceptual design

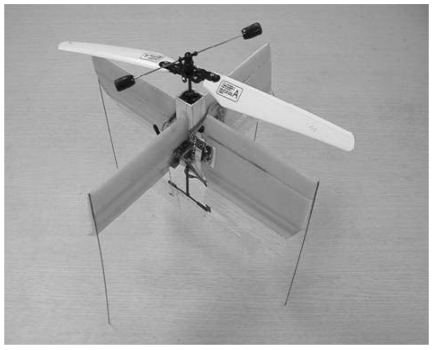

b) Final assembly

Fig. 4 Konkuk University 2004 MAV model.

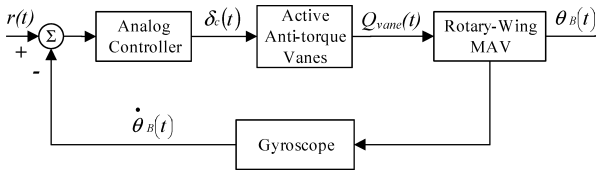

Fig. 5 Block diagram of active antitorque control system.

1900 RPM, the measured torque was about 270 gf-cm, and this value was used to design the antitorque vanes. The sizes of the antitorque vanes were determined using Eq. (9) to produce sufficient torque Q_{vane} to negate the antitorque Q_{anti},

$$Q_{\text{vane}} = \sum_{\text{passive}} \int r \, \mathrm{d}L_{\text{vane}} + \sum_{\text{acive}} \int r \, \mathrm{d}L_{\text{vane}} \tag{9}$$

$$\mathrm{d}L_{\text{vane}} = \frac{1}{2}\rho v^2 C_L c \, \mathrm{d}r \tag{10}$$

In Eq. (10), v and C_L refer to the induced velocity and the lift coefficient, respectively. The airfoil of the antitorque vane was a NACA0012. For active antitorque vanes, the control input was assumed to be 5 deg, which is one-half of the maximum value. Note that because the C_L data might be inaccurate due to a low Reynolds number and turbulence of the induced flow, we considered the torque data as a rough estimation. The 8-cm-long antitorque vanes were attached at 3.2 cm under the rotor blade to put the antitorque vanes within 12 cm under the rotor blade.

A block diagram of the control system is shown in Fig. 5. The analog controller produced the control angle proportional to the body rotation rate as measured by the gyroscope. The proportional constant was determined by a trial-and-error method. If the body of the MAV began to rotate, then a control signal produced by the gyroscope automatically prevented body rotation.

C. Flight Test

Figure 4b shows the final assembly of the rotary-wing MAV, including a video camera. An indoor flight test was performed, as shown in Fig. 6, and the demonstration is presented at URL: http://mail.konkuk.ac.kr/~nsgoo/flightest.avi (available for one year after publication). The rotary-wing MAV flew for more than 5 min. The endurance was relatively short compared to the estimated value. The relatively short endurance could have been caused by a calculation error for the discharge rate of the battery or by energy loss in the wake due to the presence of antitorque vanes. The flight was remarkably stable; therefore, we concluded that the automatic antitorque system with a gyroscope worked very well. Moreover, with the yaw direction control surface, the MAV was able to move in any direction. Therefore, it was able to approach the test target closely and capture photographs while loitering around it (URL: http://mail.konkuk.ac.kr/~nsgoo/loitering.avi).

Fig. 6 Stable flight of rotary-wing MAV.

IV. Summary

We have successfully developed a rotary-wing MAV that is powered by an electric motor and that uses an automatic antitorque control system. The developed MAV was flown for more than 5 min by radio control. Photographs taken by the installed video camera could be clearly transmitted. Though the successful flight test showed the MAV's capability for surveillance, further improvements in the propulsion system and the directional control system must be developed for forward flight during outdoor missions, where head winds and side winds will be encountered.

Acknowledgment

The authors gratefully acknowledge the financial support of Korea Research Foundation Grant KRF-2004-005-D00046.

References

[1]Grasmeyer, J. M., and Keenoon, M. T., "Development of the Black Widow Micro Air Vehicle," AIAA Paper 2001-0127, 2001.

[2]"Epson Announces Advanced Model of the World's Lightest Micr-Flying Robot," URL: http://www.epson.co.jp/e/newsroom/news_2004_08_18.htm.

[3]Bohorquz, F., Samuel, P., Sirohi, J., Pines, D., Rudd, L., and Perel, R., "Design, Analysis and Performance of a Rotary Wing MAV," *AHS Journal*, Vol. 48, No. 2, April 2003, pp. 80–90.

[4]Young, L. A., Aiken, E. W., Derby, M. R., Dembleski, R., and Navarrete, J., "Experimental investigation and Demonstration of Rotary-wing Technologies for Flight in the Atmosphere of Mars," *Proceedings of the 58th Annual Forum of American Helicopter Society*, American Helicopter Society, Alexandria, VA, June 2002.

[5]Guerrero, I., Londenberg, K., Gelhausen, P., and Myklebust, A., "A Powered Lift Aerodynamic Analysis for the Design of Ducted Fan UAVs," AIAA Paper 2003-6567, Sept. 2003.

[6]Kim, G. B., "Design, Manufacturing and Flight Test of Micro Aerial Vehicle with Rotary-Wing," MS. Thesis, Dept. of Aerospace Engineering, Konkuk Univ., Seoul, Republic of Korea, Feb. 2005 (in Korean).

[7]Gessow, A., and Myers, G. C., Jr., *Aerodynamics of the Helicopter*, Macmillan, New York, 1952, Chaps. 3, 4.

[8]Bramwell, A. R. S., *Helicopter Dynamics*, Wiley, New York, 1976, Chap. 3.